TRENDS IN SCIENCES 2026; 23(4): 11419
https://doi.org/10.48048/tis.2026.11419
RESEARCH ARTICLE

Discrimination of Seismic Signals in UGM Antenna Station Recordings at Merapi Volcano Using a Remote Seismic Array: Beamforming and FK Analysis

Dairoh[1,3], Sudarmaji[1], Ahmad Ashari[2] and Wiwit Suryanto[1,*]

[1]*Department of Physics, FMIPA, Universitas Gadjah Mada, Yogyakarta 55281, Indonesia*
[2]*Department of Computer Science and Electronics, FMIPA, Universitas Gadjah Mada, Yogyakarta 55281, Indonesia*
[3]*Informatics Engineering Study Program, Vocational School, Harkat Negeri University, Tegal 52147, Indonesia*

([*]Corresponding author's e-mail: ws@ugm.ac.id)

Received: 30 July 2025, Revised: 15 October 2025, Accepted: 1 November 2025, Published: 25 December 2025

Abstract

Effective volcano monitoring is crucial for hazard mitigation and early warning systems. This study presents a monitoring system for Merapi Volcano using 5 remote seismic stations equipped with low-cost Raspberry Shake and Boom sensors, aiming to offer an affordable alternative to conventional local monitoring networks. The objective was to evaluate the capability of the UGM (Universitas Gadjah Mada) Antenna Station Array (UAA) to detect and classify tectonic and volcanic seismic activity. The system has been operational since July 2023; however, data from only 16 August to 12 September 2023 were analysed because of initial calibration challenges affecting data reliability, mainly due to environmental and power-related factors. This study presents a pilot-scale demonstration of a low-cost remote seismic array deployed at the Merapi Volcano. Using STA/LTA detection, beamforming, and FK analysis, 376 events were identified within a 28-day dataset (August 16 - September 12, 2023). Although the short temporal coverage prevents robust statistical analysis of long-term volcanic behaviour, the results highlight the feasibility of classifying volcanic versus tectonic events from a distance of 16 km. The limitations include suboptimal array geometry, environmental calibration challenges, and a relatively high false alarm rate, underscoring the need for extended monitoring campaigns, multimodal validation, and improved signal classification. Preliminary classification was performed through comparative spectral and directional analyses. Despite the short monitoring window, results indicate the potential for focused short-term deployment to capture representative seismic behaviour during periods of increased activity. However, the limited duration does not preclude long-term trend analysis, and longer monitoring is needed to identify seasonal patterns and early signs of eruption. These findings demonstrate the potential of low-cost arrays as complementary monitoring tools in resource-limited volcanic regions, particularly for redundancy in national early warning systems.

Keywords: Merapi Volcano, Seismic, Detection, Remote and monitoring

Introduction

Merapi Volcano is among the most active volcanoes in Indonesia, with eruption intervals typically ranging from 2 to 4 years [1,2]. It is located across the Boyolali, Klaten, Magelang, and Yogyakarta regencies, with an altitude of 2,910 m above sea level [3]. Its eruptive behaviour is characterised predominantly by the growth of lava domes and incandescent lava flows, frequently accompanied by pyroclastic flows [1,2,4,5]. This volcanic activity poses significant hazards to surrounding populations and infrastructure. Given its persistent activity and proximity to densely populated areas, Merapi presents a serious threat to local communities and infrastructure. Therefore, robust and continuous monitoring is essential to mitigate volcanic risk and enhance public safety.

Current monitoring efforts rely heavily on proximal seismic stations, which are often damaged during major eruptions such as that in 2010, resulting in loss of critical data [1,2,5,6]. Furthermore, the high installation and maintenance costs of traditional dense seismic networks limit the expansion of monitoring capabilities, particularly in resource-constrained regions. These challenges underscore the need for efficient, affordable systems capable of recording high-quality data from a safe distance.

Recent developments in low-cost seismic and infrasound sensors, such as Raspberry Shake, have opened up opportunities for community-based volcano monitoring in regions with limited resources. However, most studies rely on long-term datasets that cover multiple eruptive phases. In contrast, the current study represents a pilot-scale feasibility study conducted during a 28-day deployment at Merapi Volcano. Owing to calibration issues and environmental challenges, only this truncated dataset was available for analysis. Although this limits the scope for detecting temporal or seasonal variations, the study nonetheless provides important insights into the strengths and weaknesses of low-cost seismic arrays when integrated into existing monitoring frameworks. Our aim is not to present a fully operational monitoring solution but to evaluate the prototype performance and outline the necessary steps towards operational robustness.

This study addresses this gap by demonstrating the potential of a sparse, low-cost remote seismic array previously underutilised for detailed volcanic monitoring to capture diverse seismic signals, identify their source directions, and support classification with accuracy comparable to conventional arrays. Uniquely, this research integrates standard signal processing techniques into a low-cost remote monitoring system, enabling safe and long-term seismic observation of Merapi Volcano from approximately 16 km away. Unlike previous studies relying on dense, high-cost conventional arrays, our approach shows that reliable detection and characterisation of volcanic signals can be achieved using a minimal number of affordable sensors deployed remotely.

The Universitas Gadjah Mada (UGM) has developed this low-cost remote seismic monitoring system using Raspberry Shake and Boom sensors to address these challenges. The UGM antenna station, located at Ngemplak, Sleman approximately 16 km south of Merapi's summit, comprises a vertical-component seismometer and a 5-station array spaced at 250 m. The system continuously records both seismic and infrasound signals, including during eruptive phases [7,8]. We evaluated the capability of the UGM Antenna Station to detect and characterise volcanic-tectonic (VT) events and earthquakes using STA/LTA detection, beamforming, and frequency-wavenumber (FK) analysis [9,10]. The results are expected to contribute towards the development of more reliable, economical, and extensive monitoring networks. Consequently, this approach offers a replicable, low-cost solution to enhance volcanic monitoring in high-risk regions lacking local infrastructure.

Materials and methods

Observational data on Merapi volcano

Merapi Volcano (2,910 m asl) is an active stratovolcano located in Central Java, Indonesia. The shortest eruption intervals in recent decades occurred during the significant eruptive events of 2006 and 2010 [1]. In this study, a seismic array comprising 5 stations was deployed in the Ngemplak area, Sleman, Yogyakarta Special Region, approximately 16 km south of Merapi's summit. The volcano lies a triangular to the north of the array site. The stations are arranged in a triangular configuration with approximately 250 m spacing between them (**Figure 1**).

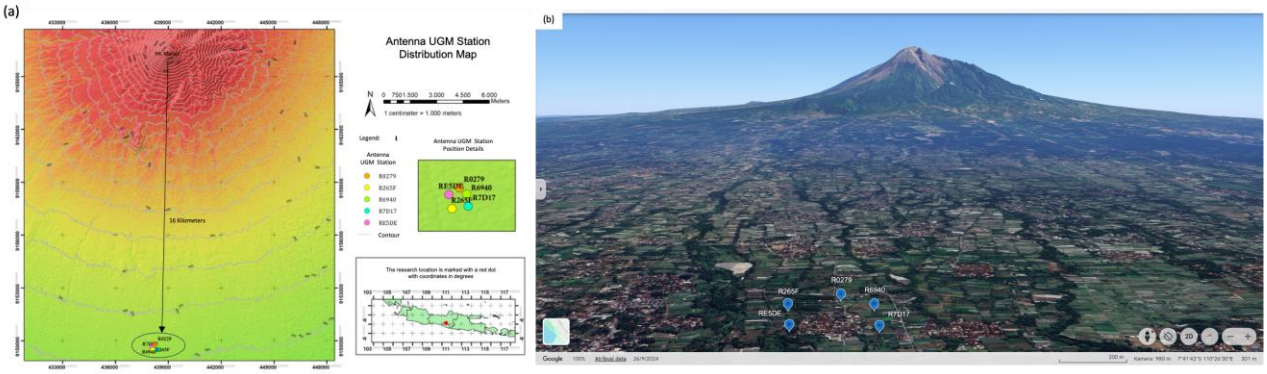

Figure 1 Distribution of UGM antenna stations (blue circles), located approximately 16 km south of the volcano. (a) Map showing station locations overlaid on a high-resolution topographic base. (b) 3D perspective view from Google Earth illustrating the spatial arrangement of UGM antenna stations in the southern lowlands relative to Merapi Volcano (Source: https://earth.google.com/).

This array was established through collaboration between Gempa GmbH and Universitas Gadjah Mada, with the aim of monitoring volcanic and tectonic events. The configuration forms a pentagonal layout (**Figure 1**), and the stations are labelled as follows: RE5DE (UGM 1), R6940 (UGM 2), R265F (UGM 3), R7D17 (UGM 4), and R0279 (UGM 5). Each station is equipped with a Raspberry Shake and Boom sensor housed within a 12-inch diameter perforated PVC cylinder, embedded in concrete blocks measuring 80×80×30 cm^3. Each seismometer (Raspberry Shake 4D) features a geophone with a corner frequency of 4.5 Hz, suitable for detecting local and regional seismic events. The analysed dataset covers this period, sampled at 100 Hz. All stations are powered by local residential electricity and transmit data via an internet connection.

It is important to note that the array geometry was not fully optimized for this deployment, which may limit its sensitivity to low-amplitude volcanic signals and to signals from distant sources. Although the pentagonal configuration was dictated by field accessibility, simulation results indicate that expanding the aperture and integrating autonomous power systems would improve azimuthal resolution and reduce data loss. Prior to commencing operation in July 2023, the UGM antenna array underwent calibration to ensure time synchronisation and power stability. However, initial data analysis revealed gaps in recordings at several stations, primarily due to unstable power supply and adverse weather conditions (e.g., strong winds, heavy rain). These calibration challenges highlight the importance of sensor maintenance and durability when operating in remote environments.

To address these issues, data synchronization and integration were performed prior to analysis. This process involved thorough inspection of daily raw recordings from all stations, following procedures similar to those described by Angelis *et al.* [7]. Synchronization ensured temporal alignment and completeness of the dataset, thereby improving the reliability of subsequent signal processing and analysis. The array records both signals (**Figure 2**).

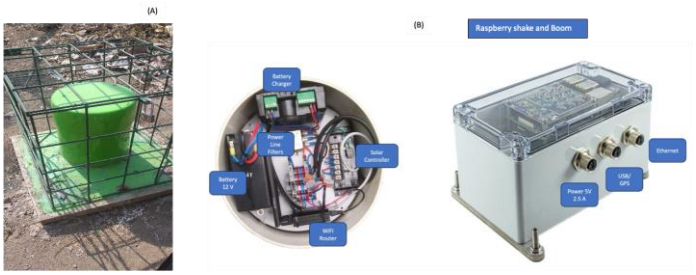

Figure 2 Field deployment of a local station at the monitoring site. (a) The physical installation of the sensor housing. (b) Internal components of the UGM antenna station, including the power supply system, solar controller, and Wi-Fi router. The Raspberry Shake device used for data acquisition is shown on the right. Although not visually depicted, a wind noise reduction system was integrated into the sensor setup during field deployment.

The synchronization results show data availability from July to December 2023 (**Figure 3(a)),** with incomplete recordings at 3 stations (R265F, R6940, and R7D17) where data availability was below 65%. This is the primary cause of data gap during period. Overall, total data availability across the 5 stations was approximately 70.04% from July to December.

By synchronising the recordings from the UGM antenna stations, a dataset spanning 16 August to 12 September 2023 was obtained with a completeness level of 99%. Consequently, this study used data from 16 August to 12 September 2023 for array processing to ensure the accuracy of estimated signal velocity and determination of the back-azimuth. This approach aligns with Rost and Thomas [10], who emphasise the importance of data quality verification and synchronisation.

The synchronisation results illustrate data availability for each station (**Figure 3**), where horizontal bars represent time intervals with valid recordings, red vertical lines indicate data gaps, cross marks denote the start of data recording, and blue lines show daily/hourly data availability.

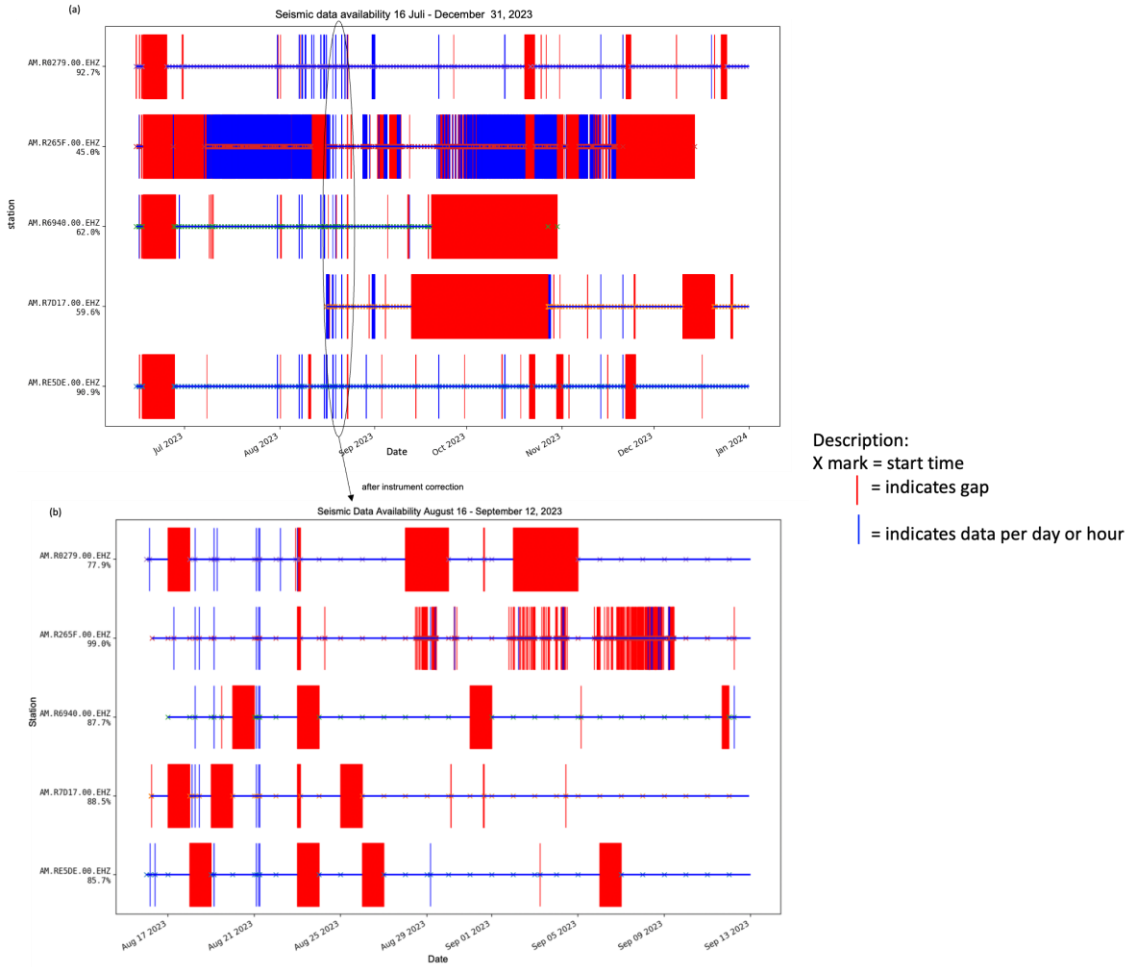

Figure 3 (a) Summary of seismic data availability from July to December 2023. (b) Final dataset used for analysis in this study, showing rectified data availability following instrumentation changes. Each station's data span 28 consecutive days, from 16 August to 12 September 2023.

Signal processing and event detection

An example of an unfiltered seismic signal recorded by an UGM antenna station is shown in **Figure 4(a)**. Seismic signal processing commenced with a Butterworth bandpass filter (0.8 - 1.8 Hz) (**Figure 4(b)**), followed by envelope extraction and smoothing using a moving median filter to suppress impulsive noise and enhance event onset clarity [11-13]. To improve the detectability of volcanic signals at the remote seismic station located 16 km from the Merapi summit, a narrow bandpass filter (0.8 - 1.8 Hz) was applied. This frequency range was selected based on the typical spectral content of low-frequency volcanic earthquakes, which generally dominate below 2 Hz due to subsurface source mechanisms [9,14].

Due to intrinsic absorption and scattering within heterogeneous volcanic media, high-frequency components are significantly attenuated at this distance[15]. Thus, focusing on the 0.8 - 1.8 Hz range reduces contamination from regional tectonic noise and anthropogenic noise (**Figure 4(c)**), while increasing the signal-to-noise ratio for volcanic events. Spectral analyses using FFT (**Figure 4(g)**) and power spectral density (PSD) were applied to evaluate the frequency characteristics of the filtered signal, complemented by root mean square (RMS) analysis to assess amplitude evolution over time [16,17]. An example PSD result is shown **Figure 4**.

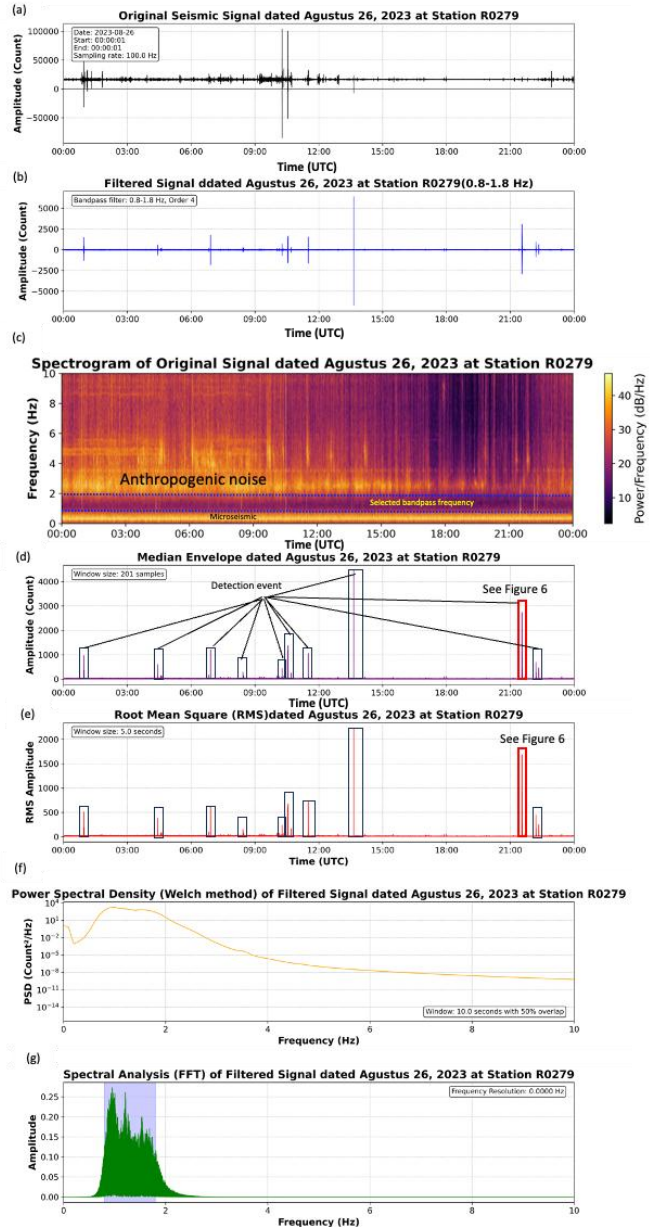

Figure 4 Seismic signal processing steps applied to the daily waveform recorded on 26 August 2023, at station R0279. (a) Raw seismic waveform with background noise and transient events (original Signal). (b) Filtered waveform using a 0.8 - 1.8 Hz Butterworth bandpass filter. (c) Spectrogram of the original signal shows persistent noise bands and the selected filter range. (d) Median envelope of the filtered signal highlighting high-energy transients. (e) RMS amplitude of the filtered signal using a 5-second window. (f) Power spectral density (PSD) illustrating dominant energy within the filter band. (g) Amplitude spectrum confirming energy concentration between 0.8 - 1.8 Hz.

Beamforming and FK analysis

Beamforming and frequency-wavenumber (FK) analysis are standard techniques used to determine the direction of arrival (DOA) and phase velocity of seismic waves. This combined approach enables enhanced detection and characterization of volcanic sources [10,24,25].

Beamforming estimates the DOA by aligning and summing waveforms across the array, based on time delays between sensors. Often presented as back azimuths, the output helps distinguish volcanic sources typically originating from the summit (0° - 30°) from more scattered tectonic sources [24,26]. This method has been effectively applied in various volcano monitoring studies, such as at Mt. Etna [10,27]. This process is described by Eq. (1):

$$B(t,s,\phi)=\frac{1}{N}\sum_{i=1}^{N}x_i(t+\tau_i(s,\phi)) \quad (1)$$

where $B\ (t, s, \emptyset)$ is the beamforming output, N is the number of sensors, $x_i(t)$ is the signal at the i-th sensor, $\tau_i(s, \emptyset)$ is the time delay, s is slowness, and $\emptyset$ is azimuth.

FK analysis complements beamforming by transforming array data into the frequency-wavenumber domain to estimate wave propagation [10,28]. Key outputs include relative power (coherency across sensors), absolute power (total signal energy), slowness (inverse wave velocity), and back azimuth (signal source direction). These parameters assist in identifying high-energy events and classifying signal types, such as distinguishing impulsive tectonic events from continuous volcanic tremors [10,12,28,29]. This study implemented both methods using seismic array data to detect and analyse volcanic activity at Merapi Volcano.

In this study, beamforming was applied to the UGM antenna station array to estimate the back azimuth of detected events, enabling discrimination between summit-originating volcanic events (0° - 30°) and more scattered tectonic events. FK analysis was then used to validate these directional estimates and quantify wave slowness, assisting in classifying impulsive versus continuous sources.

STA/LTA detection

The STA/LTA (Short-Time Average/Long-Time Average) method was applied to automatically detect seismic events [30]. Detected events were subsequently classified using waveform and spectral analyses based on established criteria [14].

$$STA/LTA(t)=\frac{STA(t)}{LTA(t)} \quad (2)$$

Statistical validation of detection performance

Standard statistical metrics, including precision, recall, and false alarm rate, were computed to evaluate the performance of the seismic signal detection and classification system. These metrics provide a quantitative assessment of the system's ability to identify true volcanic events while minimising misclassification [29,31]. Eqs. (3) - (6) represent Precision (P), Recall (R), False Alarm Rate (FAR), and Accuracy, respectively.

$$\text{Precision}=\frac{\text{TP}}{\text{TP}+\text{FP}} \quad (3)$$

$$\text{Recall}=\frac{\text{TP}}{\text{TP}+\text{FN}} \quad (4)$$

$$\text{FAR}=\frac{\text{FP}}{\text{TP}+\text{FP}} \quad (5)$$

$$\text{Accuracy}=\frac{\text{TP}+\text{TN}}{\text{TP}+\text{FP}+\text{FN}+\text{TN}} \quad (6)$$

where TP is true positives**,** FP is false positives**,** TN is the number of true negatives (correctly identified non-events) and then FN false negatives. These metrics were calculated by comparing automated detection results with a manually labelled reference catalogue based on expert review of waveform characteristics and spectrogram features [31].

This statistical framework provides an objective comparison of detection accuracy across different signal types, thresholds, or filtering approaches, consistent with previous volcano monitoring studies [31].

Validation of catalogue data

The results of the seismic signal analysis were validated using the volcanic event catalog from the Pusat Vulkanologi dan Mitigasi Bencana Geologi (PVMBG; Centre for Volcanology and Geological Hazard Mitigation) [32] and earthquake data from the Badan Meteorologi, Klimatologi, dan Geofisika (BMKG; Meteorology, Climatology, and Geophysics Agency) [33] for the period from 16 August to 12 September 2023. Validation was performed by matching event times after converting all catalogue entries to Coordinated Universal Time (UTC). According to the PVMBG catalogue, 446 volcano-tectonic (VT) events were recorded [32], while the BMKG repository documented 767 earthquakes with magnitudes ranging from 1.6 to 6.8 [34].

Results and discussion

Seismic event detection using STA/LTA algorithm

Detection and characterization were performed on all data collected during the observation period (August

16 - 12 September 2023). An example of seismic event identification and analysis conducted on 26 August 2023, is presented below. The original recorded seismic signal exhibits varying amplitudes and significant seismic activity. Its spectral properties may be linked to volcanic occurrences (Error! Reference source not found.**(a)**).

The filtered findings (Error! Reference source not found.**(b)**) retain the primary signal form while removing much background noise, thereby improving the signal-to-noise ratio, consistent with previous studies [26,35]. Filtered waveforms were automatically analysed using the STA/LTA (Short-Time Average/Long-Time Average) detection method. For instance, the signal at station R0279 was detected with an STA window of 10 seconds and an LTA window of 120 seconds. The STA/LTA algorithm triggered multiple event detections with clear onset and offset markers. Event detection applied to daily data (~8,640,000 samples; Error! Reference source not found.**(e)**) revealed a broader spectrum for detected signals compared to non-triggered signals (Error! Reference source not found.**(c) and** Error! Reference source not found.**(d)**). These results concur with prior studies demonstrating the effectiveness of STA/LTA methods for automatic volcanic activity detection [19,20,36].

Several STA/LTA-detected events were not listed in the official catalogue. Therefore, selected segments were extracted for further examination of waveform characteristics, followed by validation of the detected signals through cross-correlation analysis [16]. The identified signals exhibited cross-correlation values across 5 stations, with an average correlation coefficient of 0.78, indicating strong coherence among station pairs. These findings support previous research by Green and Neuberg [21]; Bobrov *et al.* [22]; Zavedevkin *et al.* [23], who considered cross-correlation (CC) values > 0.7 indicative of station cohesion [21-23]. Error! Reference source not found.**(e)** shows a peak correlation of 0.94 occurred at 21:00 UTC (highlighted by a yellow box), accompanied by an average correlation coefficient of 0.78 (Error! Reference source not found.**(f)**). Event detection results are summarised in Error! Reference source not found..

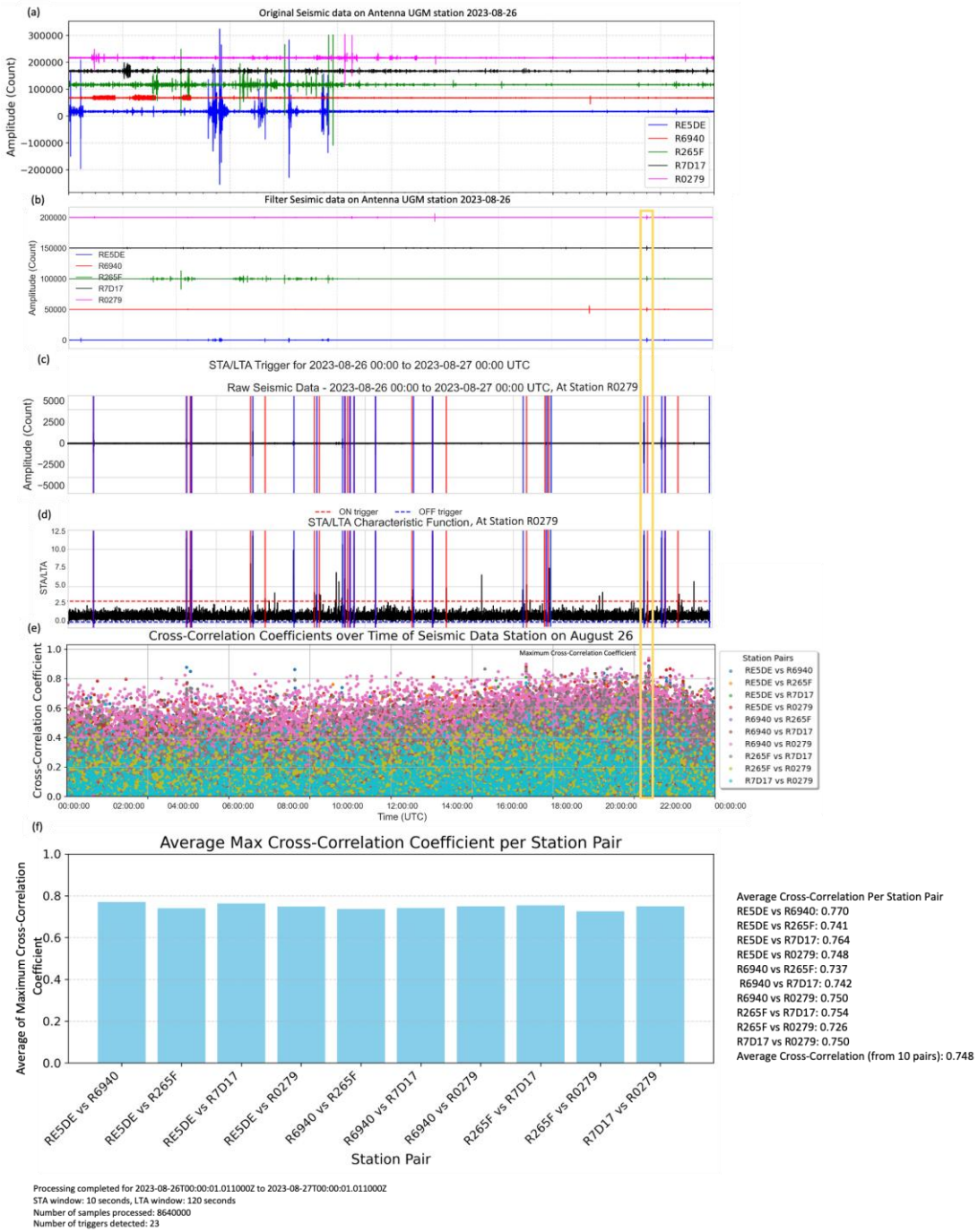

Figure 5 Multi-station analysis of seismic signals recorded on 26 August 2023, from the UGM Antenna array network. (a) Raw seismic waveform data from 5 stations: RE5DE (blue), R6940 (red), R256F (green), R7D17 (black), and R0279 (magenta). Variations in amplitude reflect both signal characteristics and local site conditions. (b) Filtered seismic data after applying a Butterworth bandpass filter (0.8 - 1.8 Hz). (c) STA/LTA event detection a station (R0279) using the short-term average (STA) to long-term average (LTA) ratio. Red vertical lines indicate trigger onset times ("ON trigger"), and blue lines indicate trigger end times ("OFF trigger"). (d) Characteristic function of STA/LTA applied to station R0279, showing detection peaks. The y-axis represents the STA/LTA ratio. Positive values correspond to high short-term signal energy relative to the long-term average. Negative values result from preprocessing artefacts; and values are clipped for clarity to highlight high signal-to-noise ratio detections. (e) Cross-correlation coefficients between all station pairs calculated from detected windows on 26 August 2023. Each dot represents the maximum cross-correlation value for a pair in a specific window. The highest observed coefficient is 0.938. (f) Average maximum cross-correlation coefficient for each pair of stations on 26 August 2023.

A total 376 tectonic volcanic events were detected using the STA/LTA detection method applied to continuous data collected from 16 August to September 12 2023. These events were verified using beamforming and FK analysis methods to confirm simultaneous wave arrivals across multiple stations.

Waveform and spectral analysis

As an example of detected events not listed in the catalogue, waveform analysis at 5 stations revealed consistent wave polarity and phase arrival times (**Figure 6(a)**), confirming simultaneous recording of the same event at all sites. This is supported by spectrograms showing dominant frequency bands in the 2 - 3 Hz range (**Figure 6(b)**), which is typical for volcanic earthquakes at Merapi Volcano [13]. Power Spectral Density (PSD) analysis further confirmed that the signals corresponded to genuine seismic activity, with signal-to-noise characteristics consistent with volcanic events (**Figure 6(c)**).

The median filter results show clear amplitude peaks, with P- and S-wave arrivals consistent with the separated signal-to-noise ratio (**Figure 6(d)**). These characteristics confirm the reliability of the STA/LTA method for detecting volcanic seismic events [19,20,36]. Overall, **Figure 6** illustrates the analysis procedure and signal characteristics obtained from STA/LTA detection.

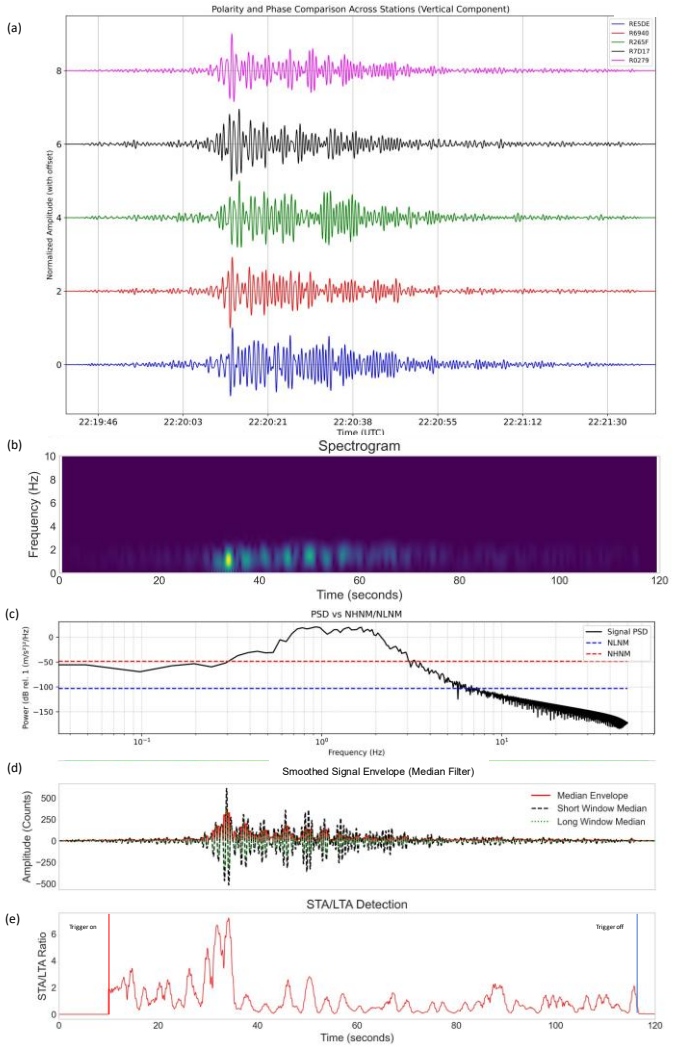

Figure 6 Characteristics of seismic signals and the automatic event detection process based on vertical component data from seismic observation stations on 26 August 2023. (a) Comparison of wave polarity and phase across several seismic stations using normalised vertical traces. (b) Spectrogram illustrating the time-frequency distribution of the signal. (c) Power Spectral Density (PSD) of a seismic signal recorded at Merapi Volcano (black line), with the New High Noise Model (NHNM, red dashed line) and New Low Noise Model (NLNM, blue dashed line) from the New Manual of Seismological Observatory Practice (NMSOP). (d) Smoothed signal envelope obtained using a median filter, highlighting significant amplitude variations. (e) Result of automatic event detection using the STA/LTA (Short-Term Average/Long-Term Average) method, indicating the estimated onset and end times of the detected event.

The detection and signal characteristics from **Figure 6** were applied to 28 days of UGM antenna station recordings, producing the dominant frequency histogram shown in **Figure 6**.

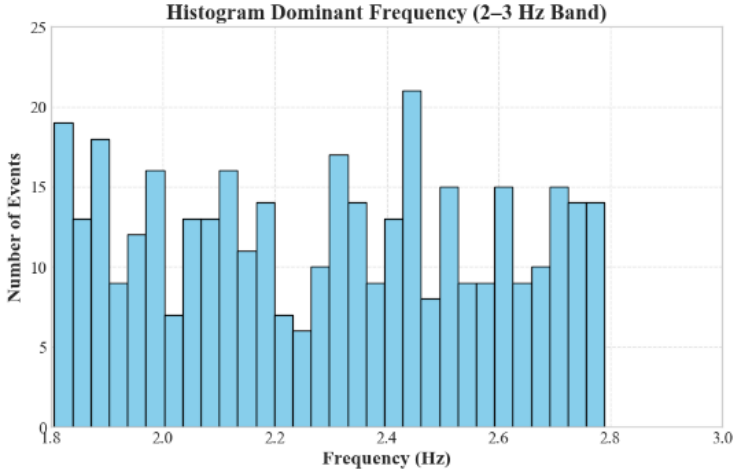

Figure 6 Histogram of dominant frequencies extracted from seismic events, showing a distribution mainly within the 2 - 3 Hz band.

Directional analysis with Beamforming and FK analysis

Beamforming and FK analysis were conducted during the data period from 16 August to 12 September 2023. **Figure 7** presents example data recorded by the UGM antenna array between 24 August and 2 September 2023.

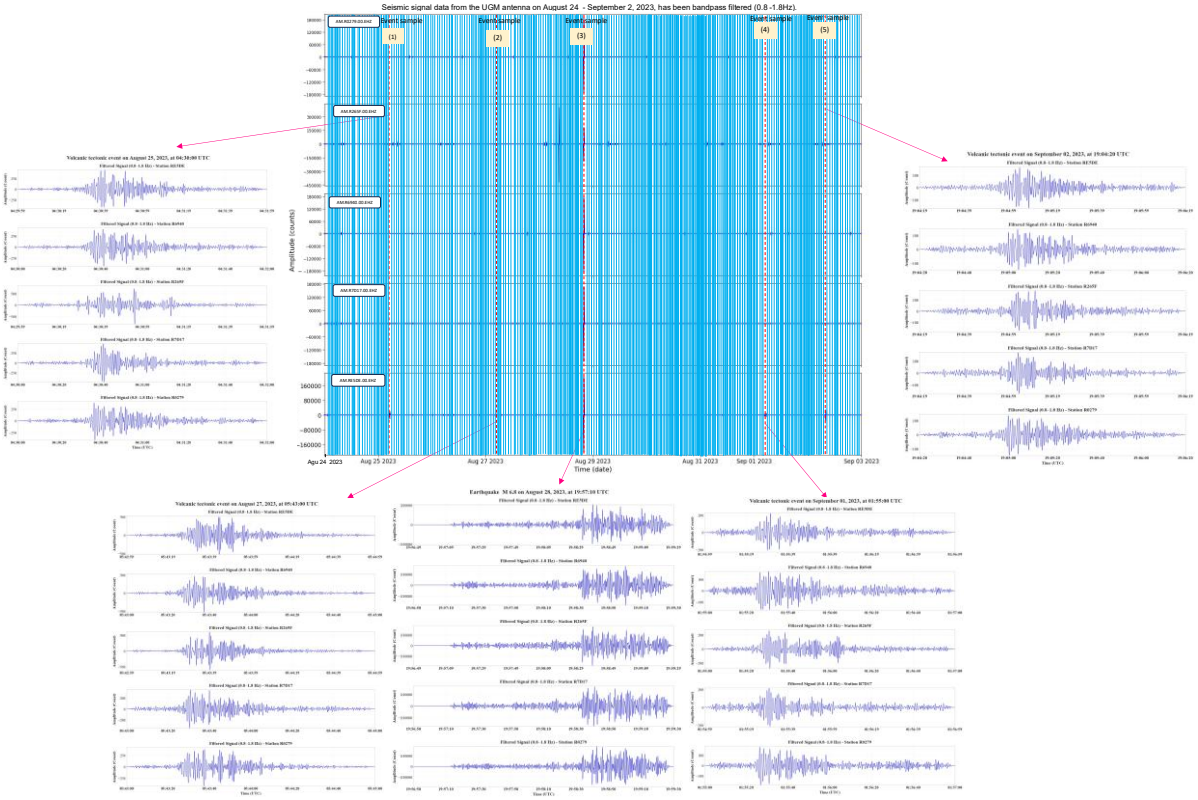

Figure 7 Example of signals recorded by the UGM antenna station from 24 August to 2 September 2023 at Merapi Volcano, filtered using a bandpass filter (0.8 - 1.8 Hz). The blue line indicates recorded events, while the red line highlights an example of a selected (cut) event.

From the analysed events (**Figure 7**), beamforming and FK analyses characterised the directional properties of STA/LTA-detected signals. For example, an earthquake with typical characteristics was detected on 5 September 2023 at 18:33:30 UTC (**Figure 8(a)**) with beamforming and FK results shown in **Figure 8** and the volcanic-tectonic event, illustrated in **Figure 9** occurred on 5 September 2023 at 17:59:47 UTC.

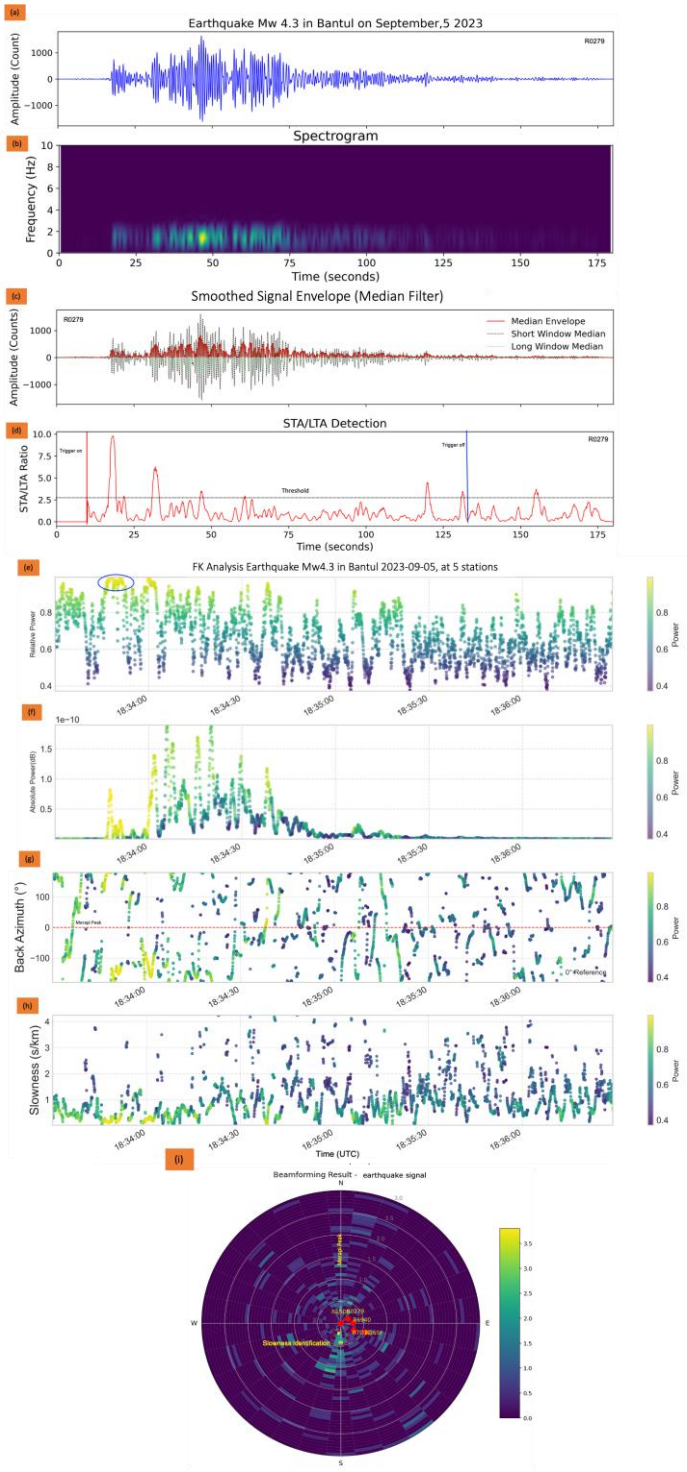

Figure 8 Illustrates analysis of the Mw 4.3 earthquake recorded at station R0279. (a) raw waveform. (b) corresponding spectrogram showing dominant frequencies. (c) smoothed envelope highlighting wave arrivals. (d) STA/LTA event detection. (e-h) FK results showing relative power, absolute power, back azimuth, and slowness. (i) beamforming polar plot indicating wave propagation direction.

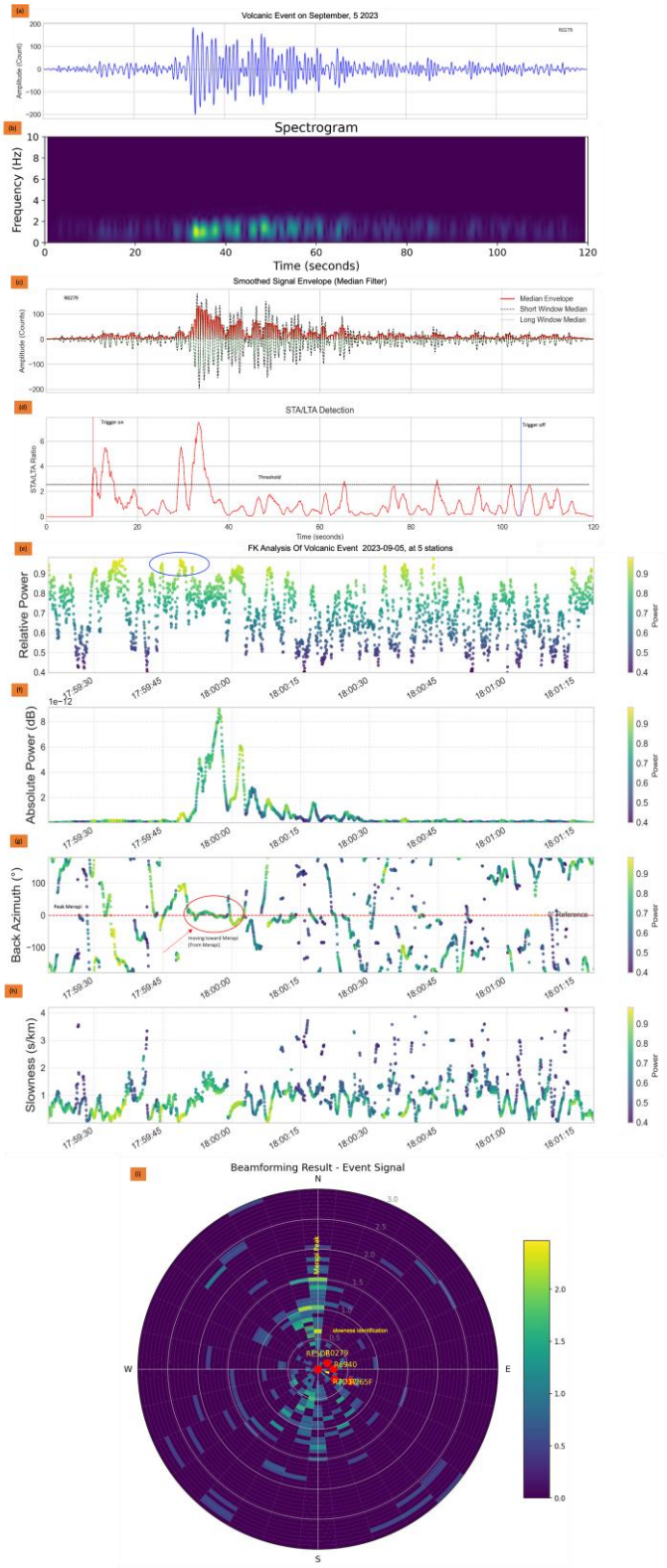

Figure 9 Analysis results of a volcanic event recorded on September 5, 2023. (a) The raw waveform of the recorded volcanic event. (b) The corresponding spectrogram shows the dominant frequency content. (c) Smoothed signal envelope using a moving median filter to suppress impulsive noise and highlight wave phase arrivals. (d) Event detection using the STA/LTA algorithm, with detection threshold indicated. (e) FK analysis results show (e) relative power, (f) absolute power, (g) back azimuth, and (h) slowness of the signal across time. (i) The beamforming result indicates the direction of wave propagation in polar coordinate.

The earthquake signal duration was approximately 60 s (**Figure 8 (b)**), whereas the volcanic tectonic event lasted about 20 s (**Figure 9**). These frequency characteristics agree with findings from [9], which show tectonic earthquakes generally have broader frequency distributions.

Beamforming and FK analysis effectively identified source directions. The earthquake exhibited a scattered azimuth with a return azimuth of 171.45°, consistent with observed apparent delays (**Figure 8 (g)**). In contrast, the volcanic tectonic event had a return azimuth of 356.67° pointing towards Merapi's summit (**Figure 9(g)**).

Further analysis confirmed slow wave velocities for earthquakes (0.3 - 0.5 s/km) and volcanic-tectonic events (0.7 - 1.2 s/km). These low velocity values indicate relatively slow earthquake wave propagation, suggesting that the earthquake sources were located at considerable distances from the observation station. These findings are consistent with the established concept that higher slowness values correlate with greater distances between the source and the array [10], while slower wave velocities combined with relatively high lag times are characteristic of shallow volcanic sources [13].

These interpretations are corroborated by BMKG catalogue data, with the earthquake event (**Figure 8)** occurring approximately 107 km offshore south of Bantul, Yogyakarta, and the volcanic tectonic event (**Figure 9**) confirmed by the PVMBG catalogue. Thus, beamforming and FK analyses provide robust estimates of seismic arrival azimuths, revealing that volcanic events predominantly originate from the northeast (aligned with Merapi's summit axis), while tectonic events show scattered azimuths.

Classification of volcanic and tectonic events

Automatic event detection using the STA/LTA algorithm, with short- and long-time windows of 10 and 120 s respectively, resulted in 376 detected events out of 446 events recorded by PVMBG (**Figure 10**), representing approximately 84.3% of the PVMBG and BMKG datasets. Seismic events were detected across 5 stations during the observation period from 16 August to 12 September 2023.

The STA/LTA detection results, combined with temporal and spectral information derived from array analysis using beamforming and FK analysis, enabled classification of tectonic signals characterised by a broader frequency range and higher apparent velocity [36,37]. In contrast, volcanic signals exhibited longer durations and lower dominant frequencies. The number of detected events varied daily, with the ratio of verified to detected events consistently exceeding 50%. This challenge in volcanic event detection has been highlighted in previous studies [20,26,29,37].

This study primarily focuses on identifying and analysing volcanic-tectonic (VT) events. Other seismic event categories [2], such as multiphase, low-frequency, or hybrid events, fall outside the scope of this work and are planned for future research as part of expanded objectives.

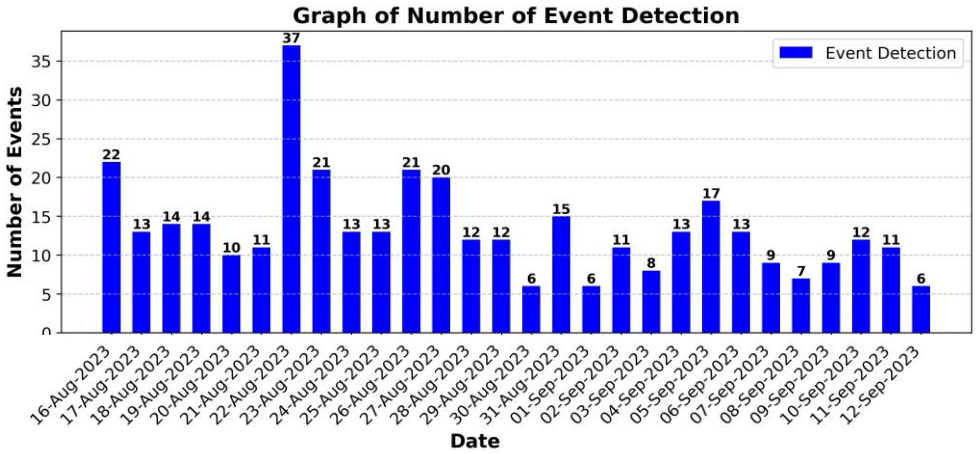

Figure 10 Number of events detected using cross-correlation and STA/LTA detection.

Quantitative performance and validation

The average cross-correlation coefficient across the 5 stations was 0.78, indicating strong signal coherence. Subsequently, statistical metrics including recall, precision, and false positive rates were evaluated to assess the volcanic event detection capability and minimise classification errors.

To support the detection results, precision, recall, and false positive rate were employed as quantitative metrics to further evaluate detection accuracy. Several standard evaluation measures were applied to quantitatively assess the performance of the proposed UGM antenna station monitoring system, as summarised in **Table 1**.

Table 1 Definition of detection metrics.

Metrics	Definition
TP	True Positive (detected & correct)
TN	True Negative (not detected & does not exist)
FP	False Positive (detected even though there is no event)
FN	False Negative (not detected even though there is an event)

These detected events were validated against the PVMBG catalogue, yielding 376 true positives (TP), 87 false positives (FP), 23 false negatives (FN), and 216 true negatives (TN). The quantitative performance of the system is summarised in **Table 2**.

Table 2 Evaluation of seismic volcanic tectonic event detection performance.

Metrics	Values
True Positive (TP)	376
False Positive (FP)	87
False Negative (FN)	23
True Negative (TN)	216
Accuracy	84.3%
Precision	81.2%
Recall	94.2%
FAR	28.7%

From the detection performance results presented in **Table 2**, it can be concluded that remote seismic monitoring using data from the UGM antenna station shows strong potential for detecting volcanic-tectonic signals. This approach can support the integration of seismic data into a multi-method monitoring framework to enhance reliability and reduce the risk of misclassification, as discussed in previous studies [6,38,39]. Accordingly, the comparison between the UGM antenna station data and the verified catalogue data is illustrated in **Figure 11**.

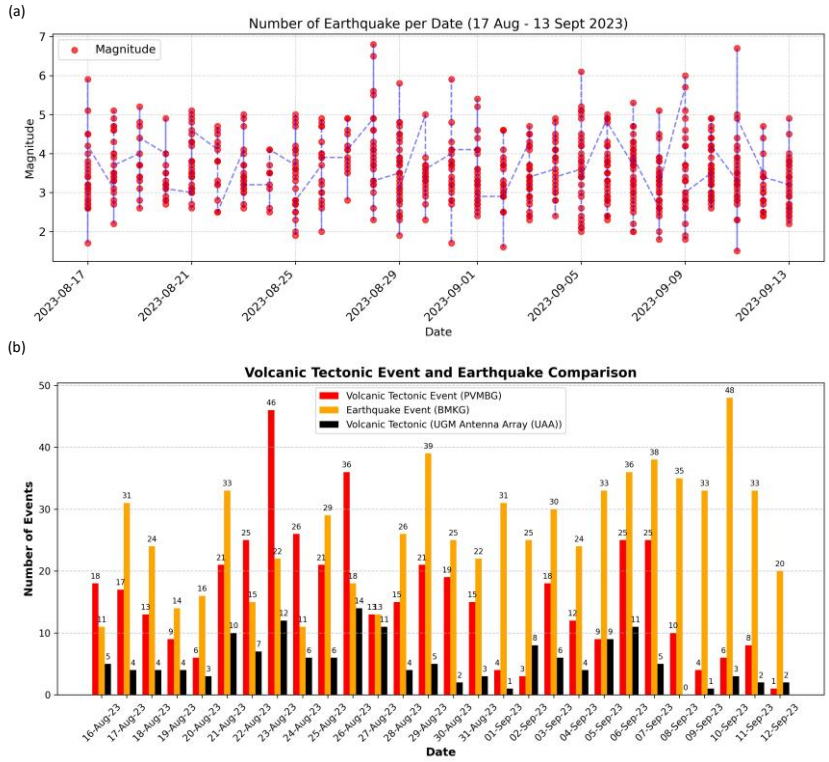

Figure 11 Comparison of volcanic and tectonic earthquake event data from multiple sources between 16 August and 12 September 2023. (a) Daily distribution of earthquake magnitudes recorded by BMKG. (b) Daily counts of volcanic-tectonic (VT) events detected at the UGM Antenna Array using FK and beamforming methods (black bars), compared with tectonic events recorded by BMKG (orange bars) and VT events reported by PVMBG (red bars). The plot highlights agreements and discrepancies among local and national observations, emphasising the utility of antenna-based detection systems for monitoring VT activity.

Integration framework, calibration challenges, and future development directions

This study highlights the importance of monitoring Merapi's volcano activity data as a solid foundation for further research, while demonstrating the potential of low-cost remote volcanic monitoring systems for operational use.

However, integrating these systems into a national monitoring protocol requires a comprehensive strategy and considerable time to overcome infrastructure challenges. This includes developing remote data access platforms, establishing reliable telemetry systems, and providing technical personnel training. Data prior to August 16 was excluded due to inconsistencies in calibrated data caused by missing data and incomplete recordings, which were due to environmental factors such as unstable power supply, strong winds, and heavy rain.

These conditions highlight the importance of routine equipment calibration and the application of noise reduction techniques to maintain data quality.

Future developments include the implementation of machine learning-based classification algorithms, extending the observation period to analyse different seasonal trends, and applying this technology to other high-risk volcanoes. Although the current dataset cannot yet distinguish all types of volcanic events, these results provide a solid foundation for developing a more comprehensive classification system, including the integration of infrasonic component signal analysis from UGM antenna stations. Future visualization and comparative analysis of seismic and infrasonic components are expected to provide deeper insights, while also opening opportunities to address data availability limitations through the deployment of additional local monitoring devices.

Discussion

STA/LTA detection can detect recording events at the UGM antenna station. Significant differences between tectonic and volcanic event signals from the station's recordings are evident in the signal characteristics shown in **Figure 8** and **Figure 9**. Earthquake signals display higher amplitudes, distinct P and S phases, a broader frequency range, and more focused wave propagation. In contrast, volcanic events exhibit more complex and scattered propagation patterns, lower amplitudes, less distinct phases, and prominent low-frequency components. These differences reflect their respective source mechanisms: Faulting for tectonic earthquakes and shallow fluid processes for volcanic events [13,37].

To quantitatively support these differences, STA/LTA analysis (Error! Reference source not found.) was applied to automatically detect volcanic tectonic events, demonstrating high sensitivity consistent with previous studies [19,20,35]. The shared source of the identified events is further confirmed by signal correlations at 5 coherent stations. These findings are in line with those of McNutt et *al.* [16]; Battaglia [39], where the identification of the same event source is strengthened by the combination of strong cross-correlation coefficients, which show both spatial and temporal cohesiveness.

Meanwhile, FK analysis **Figure 8 (h)** and **Figure 9 (h)** and beamforming **Figure 8 (i)** and **Figure 9 (i)** were utilised to differentiate the 2 event types. The result indicates that tectonic signals exhibit slower velocity vectors and back azimuth inconsistent with the Merapi peak, confirming a distant source. Conversely, volcanic events consistently show cohesive back azimuths pointing toward the summit, establishing a local volcanic origin. The reverse azimuth results demonstrate that beamforming and FK analysis can be applied to estimate the direction of seismic arrivals, consistent with the findings of Rost and Thomas [10]. From the beamforming and FK analysis results, most volcanic events originated in the northeast direction, which corresponds to the mountain peak, whereas tectonic events show more scattered azimuths. Further FK analysis confirms this trend by resolving wave velocities and azimuths in the time–frequency domain, enabling clear separation between volcanic and tectonic waves. Thus, the differences in slowness and beam power coherence also indicate a more impulsive tectonic source compared to the emergent and dispersive nature of volcanic signals [9,26,29,36].

In addition to qualitative observations, quantitative performance evaluation was conducted by comparing the detection with the PVMBG catalogue. Of 446 recorded VT events, 376 were successfully detected by the UGM antenna station. Statistical validation yielded an accuracy of 84.3%, precision of 81.2%, recall of 94.2%, and a false alarm rate (FAR) of 28.7% (**Table 2**). This evaluation confirms the method's effectiveness, particularly in detecting actual VT events while maintaining a controlled false positive rate. These results align with previous studies [29,31], indicating that statistical validation addresses the gaps identified in the last automated monitoring efforts.

Thus, the uniqueness of this study lies in the demonstration of a remote monitoring system using low-cost, university-based seismic stations applied to Merapi Volcano an approach that has not been extensively explored in prior literature. Although the results are promising, further research strategies are needed, as this study still has several limitations. The classification does not yet distinguish between different types of volcanic events (e.g., LP, tremor, and explosion), which are crucial for hazard forecasting. Nevertheless, both beamforming and FK analysis successfully distinguished tectonic and volcanic signals, even with long source-station distances.

The restricted dataset inevitably constrains the statistical robustness of the results, and our detection of VT events should be regarded as an initial proof of concept rather than an operational catalogue. Future campaigns must extend over several months to establish baselines, capture pre-eruptive signatures, and assess seasonal variability. The current pentagonal geometry, which was chosen owing to logistical constraints, provides limited resolution for back-azimuth estimation. Future designs will evaluate triangular or larger aperture configurations to improve sensitivity. Data gaps caused by unstable power supply and connectivity further emphasize the need for redundant systems, including solar backup, weatherproof housing, and data buffering. The observed data gaps and environmental susceptibilities underline the prototype nature of the current system. To enhance its operational robustness, several engineering improvements are proposed. These

include the implementation of weatherproof sensor enclosures to reduce moisture ingress and wind interference, the integration of solar power backup systems to maintain continuous operation during grid instability, and the development of automated data quality control algorithms to detect and flag corrupted or missing records in real time. Furthermore, establishing redundant local and cloud-based data storage would improve reliability and prevent data loss. In addition, future deployments will prioritise seismologically optimised sensor placement based on expected source azimuths, local topography, and noise conditions, rather than solely logistical accessibility. These measures represent the next steps toward transforming the prototype network into a sustainable, deployment-ready monitoring system suitable for continuous volcano surveillance.

The relatively high false alarm rate (28.7%) also highlights the importance of integrating independent data streams, such as infrasound, thermal imagery, and visual observations, and applying more advanced classification approaches (CNN, LSTM, and attention-based models) to reduce false positives while capturing a broader spectrum of events, including LP, hybrid, and tremor events.

Therefore, this study provides findings to strengthen the potential of combining array-based infrasound and seismic monitoring for real-time classification of volcanic and tectonic events, especially in areas with difficult access or limited station coverage [10]. The novelty lies in demonstrating a localized hybrid system based on Raspberry Shake and Boom sensors operated by a university-based network an approach with substantial potential for cost-effective volcanic monitoring in developing regions.

In this study, false positives remain a notable issue, particularly those arising from non-volcanic sources. Classification errors could be further reduced through spectral–temporal feature extraction and the application of machine learning–based classification. Expanding the spatial distribution of sensors, improving denoising methods, and enhancing real-time data processing can also improve detection capabilities. Future studies should additionally consider long-term monitoring to analyse temporal patterns and enhance resilience against seasonal environmental noise. Given the reliance on a low-cost monitoring network, this study underscores the importance of implementing scheduled calibration protocols and incorporating redundancy in station placement to enhance data reliability and resilience against environmental degradation.

Conclusions

This study demonstrates that combining beamforming and FK analysis enables effective detection and classification of seismic signals using a local seismic array. Beamforming provides accurate estimates of signal direction, while FK analysis facilitates differentiation of wave types and propagation characteristics. Together, these methods successfully differentiate between tectonic and volcanic signals, identifying 376 volcanic events that correspond with the PVMBG catalogue, achieving a validation accuracy of 84.3%.

The main contribution lies in proving the feasibility of a cost-effective, university-operated array 16 km from Merapi Volcano for reliable volcanic event detection. This supports the potential of low-cost, remote arrays as complementary tools for official monitoring networks in resource-limited regions.

This study also demonstrates the feasibility of discriminating between volcanic and tectonic events at Merapi Volcano using a low-cost seismic array. However, it also reveals significant limitations that must be addressed before such systems can be considered operational in the field. The short observation period, suboptimal geometry, calibration challenges, and relatively high false alarm rate collectively highlight the prototype nature of the current deployment. To move toward operational adoption, future studies must include extended monitoring, optimized array design, robust calibration protocols, and integration with multimodal datasets. Importantly, a clear implementation roadmap is required for integration into PVMBG monitoring protocols, including data standards, quality control procedures, and personnel training. Quantitative benchmarking against existing national networks will help identify the specific operational niches where low-cost arrays provide genuine added value, such as redundancy during sensor failures or community-based deployment. These steps will ensure that low-cost arrays

evolve from experimental demonstrations to reliable components of volcano early-warning systems.

Despite these promising results, limitations remain in this study, including the geometry and density of stations limited to the current array, which restricts the resolution of source localization. Moreover, the system does not yet provide multi-type volcanic event classification (e.g., long-period events, tremors, explosions), and validation relied solely on seismic catalogues without cross-verification from visual or geochemical observations.

Future work will integrate supervised and unsupervised machine learning techniques to enhance detection accuracy and enable multi-class event classification without manual labelling. Additional developments will include spectral–temporal feature extraction, real-time data processing, and expansion of spatial coverage through further station deployments, all aimed at improving system robustness and monitoring effectiveness.

Acknowledgments

The researchers would like to thank Gempa GmbH for the collaboration on the installation and installation of the UGM Antenna station equipment.

Declaration of generative AI in scientific writing

During the preparation of this manuscript, the author(s) used Grammarly and Claude in order to correct the grammar, spelling, and readability of the manuscript Following the application of this tool/service, the author(s) thoroughly reviewed and edited the content as necessary and take full responsibility for the final published version.

CRediT author statement

Dairoh: Conceptualization, Data curation, Methodology, Project administration, Resources Investigation, Writing original draft, and Visualization; **Sudarmaji**: Supervision, Validation, and Writing review & editing; **Ahmad Ashari**: Data curation, Formal analysis, and Investigation; **Wiwit Suryanto**: Conceptualization, Supervision, Project administration, Validation, Writing review & editing and Funding acquisition.

Data availability information

The seismic station data used in the research was recorded from UGM antenna station. Then the volcanic events catalogue data is taken from the official Merapi activity report owned by the Pusat Vulkanologi dan Mitigas Bencana Geologi (PVMBG) or Center for Volcanology and Geological Disaster Mitigation through Magma Indonesia on the page https://magma .esdm.go.id/ While the earthquake catalogue data used from the Badan Meteorology, Klimatologi dan Geofisika (Meteorology, Climatology, and Geophysics Agency) (BMKG) which is available in the BMKG repository at https://repogempa.bmkg.go.id/.

References

[1] P Jousset, J Pallister, M Boichu, MF Buongiorno, A Budisantoso, F Costa, S Andreastuti, F Prata, D Schneider, L Clarisse, H Humaida, S Sumarti, C Bignami, J Griswold, S Carn, C Oppenheimer and F Lavigne. The 2010 explosive eruption of Java's Merapi volcano - A '100-year' event. *Journal of Volcanology and Geothermal Research* 2012; **241**, 121-135.

[2] A Ratdomopurbo and G Poupinet. An overview of the seismicity of merapi volcano (Java, Indonesia). *Journal of Volcanology and Geothermal Research* 2000; **100(1-4)**, 193-214.

[3] Pusat Vulkanologi dan Mitigasi Bencana Geologi. *Data dasar gunung api indonesia, dalam, data dasar gunung api Indonesia* (*in Indonesian*). Pusat Vulkanologi dan Mitigasi Bencana Geologi, Bandung, Indonesia, 2014

[4] B Voight, EK Constantine, S Siswowidjoyo and R Torley. Historical eruptions of Merapi Volcano, Central Java, Indonesia, 1768-1998. *Journal of Volcanology and Geothermal Research* 2000; **100(1-4)**, 69-138.

[5] JC Komorowski, S Jenkins, PJ Baxter, A Picquout, F Lavigne, S Charbonnier, R Gertisser, K Preece, N Cholik, A Budi-Santoso and Surono. Paroxysmal dome explosion during the Merapi 2010 eruption: Processes and facies relationships of associated high-energy pyroclastic density currents. *Journal of Volcanology and Geothermal Research* 2013; **261**, 260-294.

[6] A Budi-Santoso, P Lesage, S Dwiyono, Sri Sumarti, Subandriyo, Surono, P Jousset and JP

Metaxian. Analysis of the seismic activity associated with the 2010 eruption of Merapi Volcano, Java. *Journal of Volcanology and Geothermal Research* 2013; **261**, 153-170.

[7] S De Angelis, L Zuccarello, S Rapisarda and V Minio. Introduction to a community dataset from an infrasound array experiment at Mt. Etna, Italy. *Scientific Data* 2021; **8(1)**, 247.

[8] D Fee, SR McNutt, TM Lopez, KM Arnoult, CAL Szuberla and JV Olson. Combining local and remote infrasound recordings from the 2009 Redoubt Volcano eruption. *Journal of Volcanology and Geothermal Research* 2013; **259**, 100-114.

[9] BA Chouet and RS Matoza. A multi-decadal view of seismic methods for detecting precursors of magma movement and eruption. *Journal of Volcanology and Geothermal Research* 2013; **252**, 108-175.

[10] S Rost and C Thomas. Array seismology: Methods and applications. *Reviews of Geophysics* 2002; **40(3)**, 2-1.

[11] WD Stanley, GR Dougherty, R Dougherty and H Saunders. Digital signal processing (2nd edition). *Journal of Vibration, Acoustics, Stress, and Reliability* 1988; **110(1)**, 126-127.

[12] F Scherbaum. *Of poles and zeros: Fundamentals of digital seismology*. Springer, London, England, 2006.

[13] J Wassermann. Volcano seismology. *New Manual of Seismological Observatory Practice* 2012; **2**, 1-77.

[14] SR Mcnutt. Volcanic seismology. *Annual Review of Earth and Planetary Sciences* 2005; **33(1)**, 461-491.

[15] U Wegler and BG Lühr. Scattering behaviour at Merapi Volcano (Java) revealed from an active seismic experiment. *Geophysical Journal International* 2001; **145(3)**, 579-592.

[16] SR McNutt, G Thompson, ME West, D Fee, S Stihler and E Clark. Local seismic and infrasound observations of the 2009 explosive eruptions of Redoubt Volcano, Alaska. *Journal of Volcanology and Geothermal Research* 2013; **259**, 63-76.

[17] NE Helwig, S Hong and ETH Wecksler. *Digital signal processing, fundamentals and applications*. Academic Press, Oxford, United Kingdom, 2008.

[18] S Gentili and A Michelini. Automatic picking of P and S phases using a neural tree. *Journal of Seismology* 2006; **10(1)**, 39-63.

[19] RS Jakka and S Garg. Understanding and parameter setting of STA/LTA trigger algorithm. *Earthquake Engineering and Engineering Vibration* 2015; **14**, 27-35.

[20] Y Vaezi and M van der Baan. Comparison of the STA/LTA and power spectral density methods for microseismic event detection. *Geophysical Journal International* 2015; **203(3)**, 1896-1908.

[21] DN Green and J Neuberg. Seismic and infrasonic signals associated with an unusual collapse event at the Soufrière Hills volcano, Montserrat. *Geophysical Research Letters* 2005; **32(7)**, L07308.

[22] D Bobrov, I Kitov and L Zerbo. Perspective of cross correlation in seismic monitoring at the International Data Center. *Pure and Applied Geophysics* 2014; **171(3)**, 439-468.

[23] IA Zavedevkin, AA Shakirova and PP Firstov. DrumCorr program for selecting volcanic event multiplets based on cross-correlation analysis. *Journal of Physics: Conference Series* 2021; **2094(3)**, 032048.

[24] K Yamakawa, M Ichihara, K Ishii, H Aoyama, T Nishimura and M Ripepe. Azimuth estimations from a small aperture infrasonic array: Test observations at Stromboli Volcano, Italy. *Geophysical Research Letters* 2018; **45(17)**, 8931-8938.

[25] F Biagioli, JP Métaxian, E Stutzmann, M Ripepe, P Bernard, A Trabattoni, R Longo and M Bouin. Array analysis of seismo-volcanic activity with distributed acoustic sensing. *Geophysical Journal International* 2024; **236(1)**, 607-620.

[26] J Li, M He, G Cui, X Wang, W Wang and J Wang. A novel method of seismic signal detection using waveform features. *Applied Sciences* 2020; **10(8)**, 2919.

[27] A Cannata, G Di Grazia, M Aliotta, C Cassisi, P Montalto and D Patanè. Monitoring seismo-volcanic and infrasonic signals at volcanoes: Mt. Etna case study. *Pure and Applied Geophysics* 2013; **170(11)**, 1751-1771.

[28] J Capon. High-resolution frequency-wavenumber spectrum analysis. *Proceedings Of the IEEE* 1969; **57(8)**, 1408-1418.

[29] RS Matoza, DN Green, A Le Pichon, PM Shearer, D Fee, P Mialle and L Ceranna. Automated detection and cataloging of global explosive volcanism using the International Monitoring System infrasound network. *Journal of Geophysical Research: Solid Earth* 2017; **122(4)**, 2946-2971.

[30] A Trnkoczy. *Understanding and parameter setting of STA/LTA trigger algorithm*. *In*: P Bormann (Ed.). New manual of seismological observatory practice. GeoForschungsZentrum, Potsdam, Germany, 2009.

[31] J Davis and M Goadrich. The relationship between precision-recall and ROC curves. *In*: Proceedings of the 23rd International Conference on Machine Learning. New York, United States, 2006, p. 233-240.

[32] PVMBG. *Magma Indonesia pusat vulkanologi dan mitigasi bencana geology* (*in Indonesian*), Available at: https://magma.vsi.esdm.go.id/, accessed May 2024.

[33] BMKG. Repository, Available at: https://repogempa.bmkg.go.id/, accessed May 2024.

[34] BMKG. Badan Meteorologi Klimatologi dan Geofisika (*in Indonesian*), Available at: https://www.bmkg.go.id/, accessed May 2024.

[35] A Rakhman, Wahyudi, A Budi Santoso, H Humaida and W Suryanto. Ambient seismic noise analysis associated with the 2010 eruption of merapi volcano using temporal variations of randomness and background noise. *International Journal of Geophysics* 2020; **2020(1)**, 8853376.

[36] L Küperkoch, T Meier, J Lee, W Friederich and EGELADOS Working Group. Automated determination of p-phase arrival time at regional and local distances using higher order statistics. *Geophysical Journal International* 2010; **181(2)**, 1159-1170.

[37] J Neuberg, R Luckett, B Baptie and K Olsen. Models of tremor and low-frequency earthquake swarms on Montserrat. *Journal of Volcanology and Geothermal Research* 2000; **101(1-2)**, 83-104.

[38] DC Roman and KV Cashman. The origin of volcano-tectonic earthquake swarms. *Geology* 2006; **34(6)**, 457-460.

[39] J Battaglia. Location of seismic events and eruptive fissures on the piton de la fournaise volcano using seismic amplitudes. *Journal of Geophysical Research: Solid Earth* 2003; **108(B8)**, 2364.